# Small-sized and high-dispersed Pt nanoparticles loading on graphite nanoplatelets as an effective catalyst for methanol oxidation

Genlei Zhang[a], Zhenzhen Yang[b], Chengde Huang[c], Wen Zhang[a], and Yuxin Wang[a,] *

[a] School of Chemical Engineering and Technology, State Key Laboratory of Chemical Engineering, Co-Innovation Center of Chemical Science & Engineering, Tianjin Key Laboratory of Membrane Science and Desalination Technology, Tianjin University, Weijin Road, Tianjin 300072, PR China

[b] School of Chemical Engineering and Technology, State Key Laboratory of Chemical Engineering, Co-Innovation Center of Chemical Science & Engineering, Tianjin University, Weijin Road, Tianjin 300072, PR China

[c] School of Chemical Engineering and Technology, Department of Applied Chemistry, Tianjin University, Weijin Road, Tianjin 300072, PR China

# 1. Electrochemical impedance measurements.

The electrochemical impedance spectra (EIS) were recorded at the frequency range from 100 kHz to 10 mHz with 10 points per decade. The amplitude of the sinusoidal potential signal was 5 mV.

Electrochemical impedance spectroscopy (EIS) has been used to characterize methanol oxidation electrocatalytic activities. In the Nyquist plot, there are usually two semicircles associated with electrochemical activities on anode surface. The high frequency semicircle represents a charge transfer process, whereas the other in the low frequency region sometimes demonstrates inductive behavior related to certain adsorption processes.[1] Methanol oxidation on the Pt surface is a surface structure-sensitive process, which involves several complicated intermediate reactions.[2] A large diameter in the Nyquist plot indicates a large Faradaic resistance, which corresponds to a low methanol oxidation current density. In other reports, low frequency impedance spectrum sometimes appears in the fourth quadrant as the behavior of inductance.[3] Inductive characteristics are related to the adsorption of $CO_{ads}$ on the catalyst surface, the removal of $CO_{ads}$ through the reaction with $OH_{ads}$, and the slow coverage relaxation of $CO_{ads}$.

## 2 Supporting Tables and Figures.

**Table S1** Summary of loading date for the catalysts on the basis of ICP-OES analysis.

| Samples | Pt (wt%) |
|---|---|
| Pt/I-IL (0)/GNPs | 12.55 |
| Pt/I-IL (2.5)/GNPs | 14.97 |
| Pt/I-IL (5.0)/GNPs | 17.32 |
| Pt/I-IL (10)/GNPs | 19.41 |
| Pt/I-IL (15)/GNPs | 18.73 |
| Pt/I-IL (20)/GNPs | 18.02 |

**Table S2** Particle size and electrochemical surface area (ECSA) estimated from hydrogen absorption comparison for Pt/I-IL (x)/GNPs catalysts used in this work.

| Samples | Particles Size / nm | ECSA / $m^2$ $g^{-1}$ |
|---|---|---|
| Pt/I-IL (0)/GNPs | 4.07 | 54.13 |
| Pt/I-IL (2.5)/GNPs | 4.00 | 58.58 |
| Pt/I-IL (5.0)/GNPs | 2.69 | 68.13 |
| Pt/I-IL (10)/GNPs | 1.94 | 73.61 |
| Pt/I-IL (15)/GNPs | 2.16 | 69.24 |
| Pt/I-IL (20)/GNPs | 3.18 | 65.7 |
| Pt/C-JM | 2.25 | 62.03 |

**Table S**3 Mass activity and specific activity expressed as the positive scan peak current for Pt/I-IL (x)/GNPs catalysts in 0.5 M $H_2SO_4$ containing 1 M $CH_3OH$.

| Samples | Mass Activity / A $g^{-1}_{Pt}$ | Specific Activity / mA $cm^{-2}$ |
|---|---|---|
| Pt/I-IL (0)/GNPs | 267.41 | 4.34 |
| Pt/I-IL (2.5)/GNPs | 404.06 | 6.66 |
| Pt/I-IL (5.0)/GNPs | 883.73 | 14.57 |
| Pt/I-IL (10)/GNPs | 1559.69 | 25.71 |
| Pt/I-IL (15)/GNPs | 971.12 | 16.01 |
| Pt/I-IL (20)/GNPs | 746.39 | 12.30 |
| Pt/C-JM | 567.15 | 9.35 |

**Table S4** The positive scan peak current density normalized as specific activity and mass activity for the Pt/I-IL (10)/GNPs catalyst and other recently reported catalysts.

| Catalysts | Specific Activity ($mA\ cm^{-2}$) | Mass Activity ($A\ g^{-1}_{Pt}$) | Scanning rate ($mV\ s^{-1}$) | Condition | Ref. |
|---|---|---|---|---|---|
| Pt/I-IL (10)/GNPs | 34.28 | 1559.7 | 50 | 0.5 M $H_2SO_4$ + 1 M $CH_3OH$ | This work |
| Pt-$Ni_2P$/C-30% | 4.05 | 1432 | 50 | 0.5 M $H_2SO_4$ + 1 M $CH_3OH$ | [4] |
| Pt-WC/graphene | | 687 | 50 | 1 M $H_2SO_4$ + 1 M $CH_3OH$ | [5] |
| TP-BNGN | | 647.2 | 50 | 0.5 M $H_2SO_4$ + 0.5 M $CH_3OH$ | [6] |
| Pt/$MnO_x$-PEDOT-MWCNTs | | 585.1 | 50 | 0.5 M $H_2SO_4$ + 0.5 M $CH_3OH$ | [7] |
| Pt-PSS-G | | 539.2 | 50 | 0.5 M $H_2SO_4$ + 0.5 M $CH_3OH$ | [8] |
| Pt-WN/graphene | | 531.5 | 50 | 1 M $H_2SO_4$ + 1 M $CH_3OH$ | [9] |
| Pt NC-CNTs | 0.82 | 530 | 50 | 0.5 M $H_2SO_4$ + 1 M $CH_3OH$ | [10] |
| PtPd/C nanowire | | 526.1 | 50 | 0.5 M $H_2SO_4$ + 0.5 M $CH_3OH$ | [11] |
| $Pt_2Au_1$/graphene | | 394 | 50 | 0.5 M $H_2SO_4$ + 0.5 M $CH_3OH$ | [12] |
| Pt/GS (31 wt%) | 22.1 | 202.2 | 20 | 0.5 M $H_2SO_4$ + 1 M $CH_3OH$ | [13] |
| Pt NPs@G | | 195 | 10 | 0.5 M $H_2SO_4$ + 1 M $CH_3OH$ | [14] |
| Pt/CNT-PIL | | 155.7 | 50 | 0.5 M $H_2SO_4$ + 1 M $CH_3OH$ | [15] |

**Table S5** Dependence of the enhancement factor R on different potentials.

| Pontential / V | R | |
|---|---|---|
| | Pt/I-IL (10)/GNPs *vs.* Pt/I-IL (0)/GNPs | Pt/I-IL (10)/GNPs *vs.* Pt/C-JM |
| 0.4 | 9.09 | 5.09 |
| 0.5 | 11.04 | 5.57 |
| 0.6 | 13.23 | 6.06 |
| 0.7 | 11.12 | 5.44 |
| 0.8 | 10.49 | 5.05 |

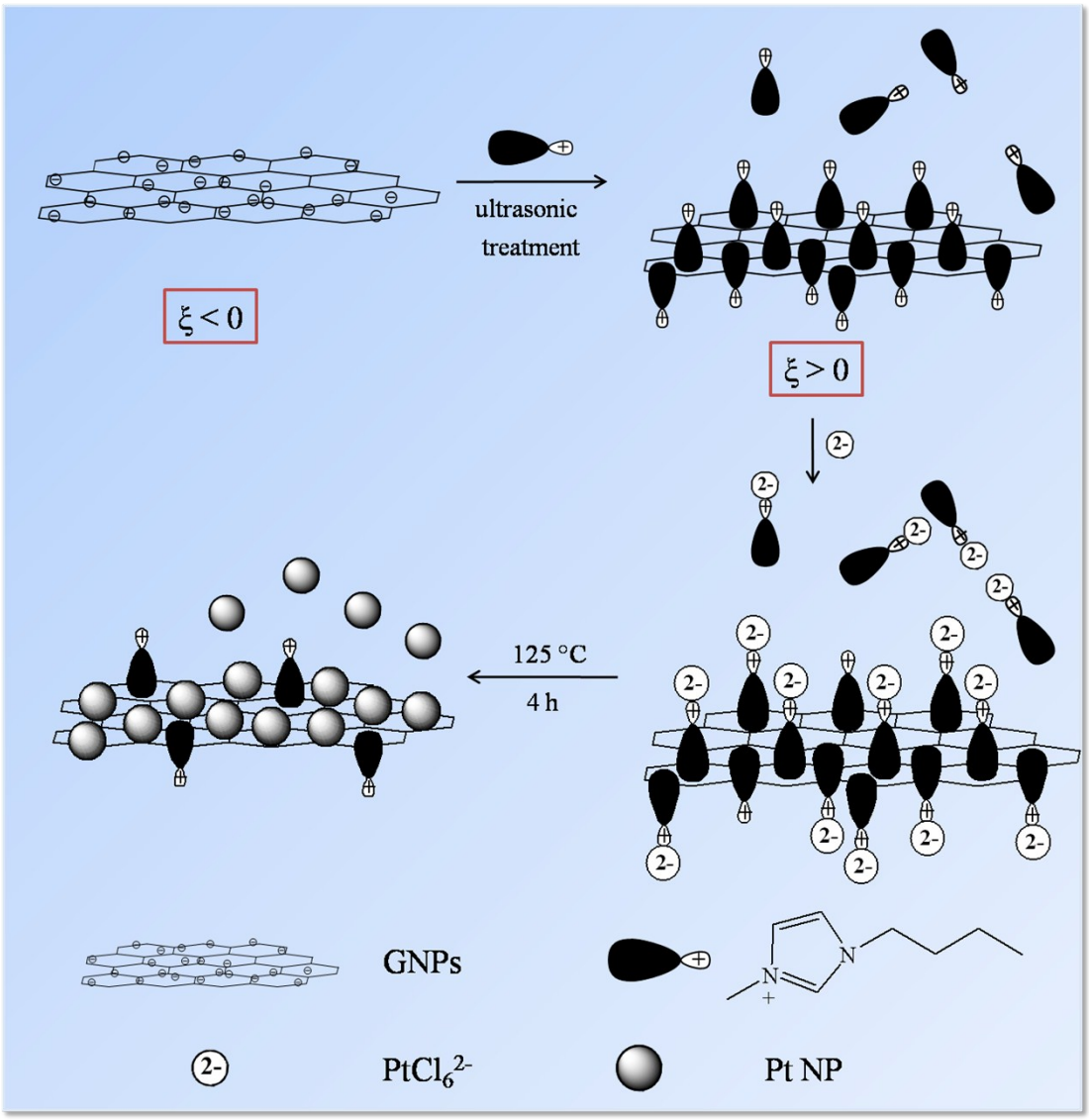


**Scheme S1** Illustration of the procedure for preparing Pt/I-IL/GNPs catalyst when IL is excess. ξ is zeta potential.

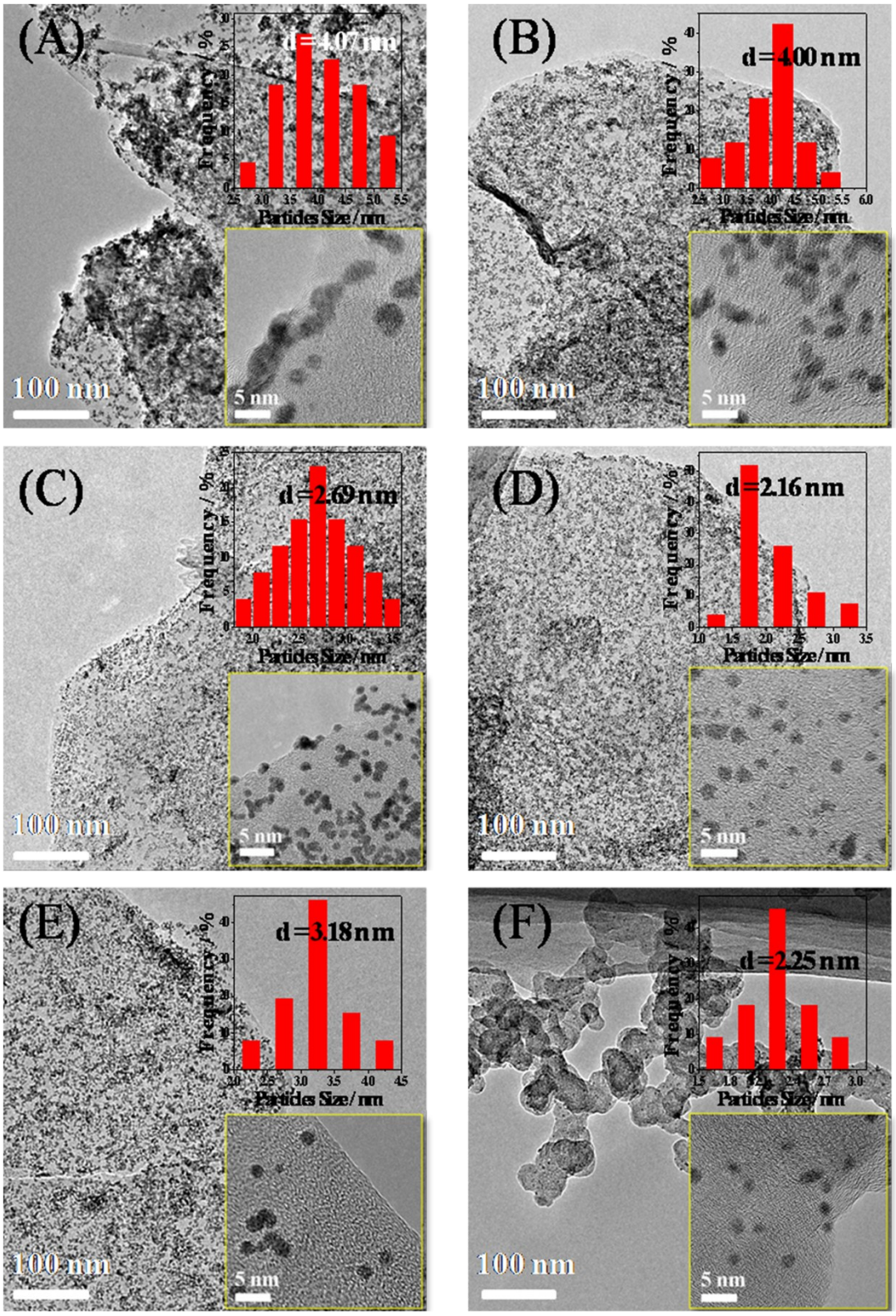


**Figure S1** TEM for (A) Pt/I-IL (0)/GNPs, (B) Pt/I-IL (2.5)/GNPs, (C) Pt/I-IL (5.0)/GNPs, (D) Pt/I-IL (15)/GNPs, (E) Pt/I-IL (20)/GNPs and (F) Pt/C-JM catalysts. Insets are the corresponding particle size distribution histograms and HRTEM images.

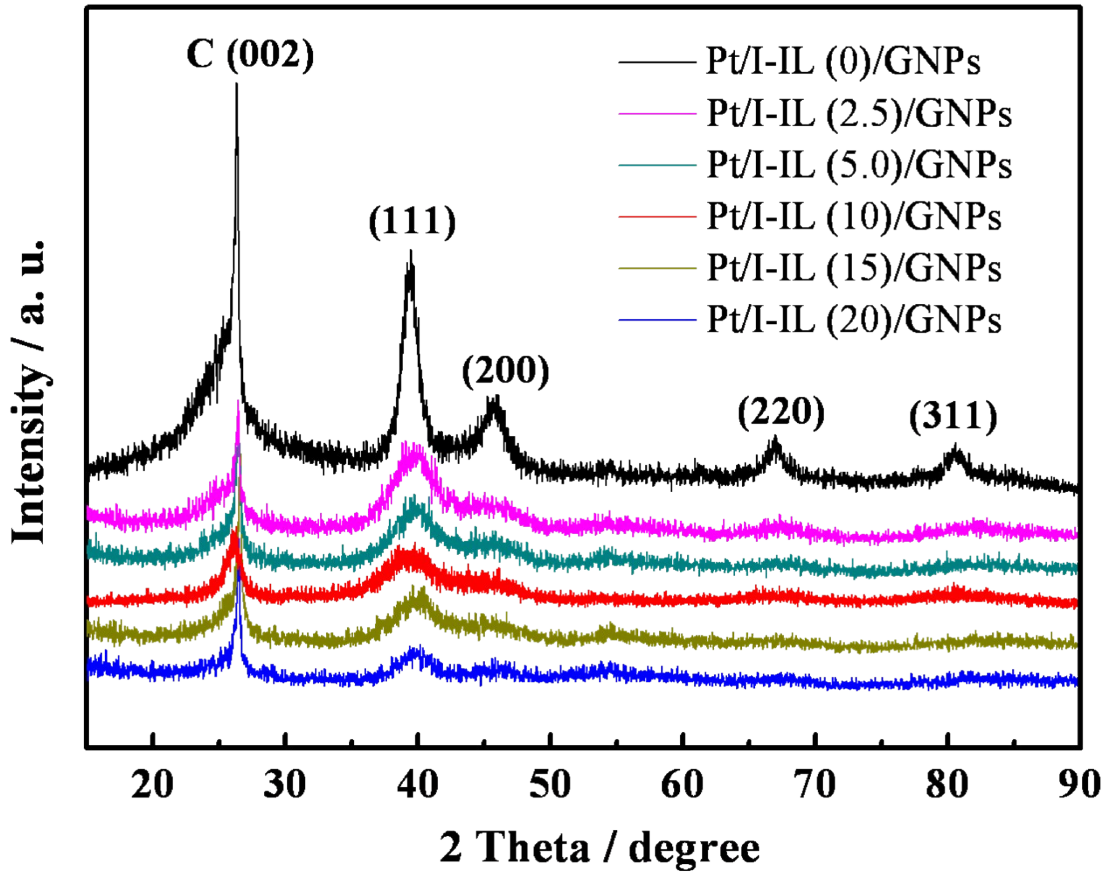


**Figure S2** XRD patterns of Pt/I-IL (0)/GNPs, Pt/I-IL (2.5)/GNPs, Pt/I-IL (5.0)/GNPs, Pt/I-IL (10)/GNPs, Pt/I-IL (15)/GNPs and Pt/I-IL (20)/GNPs catalysts.

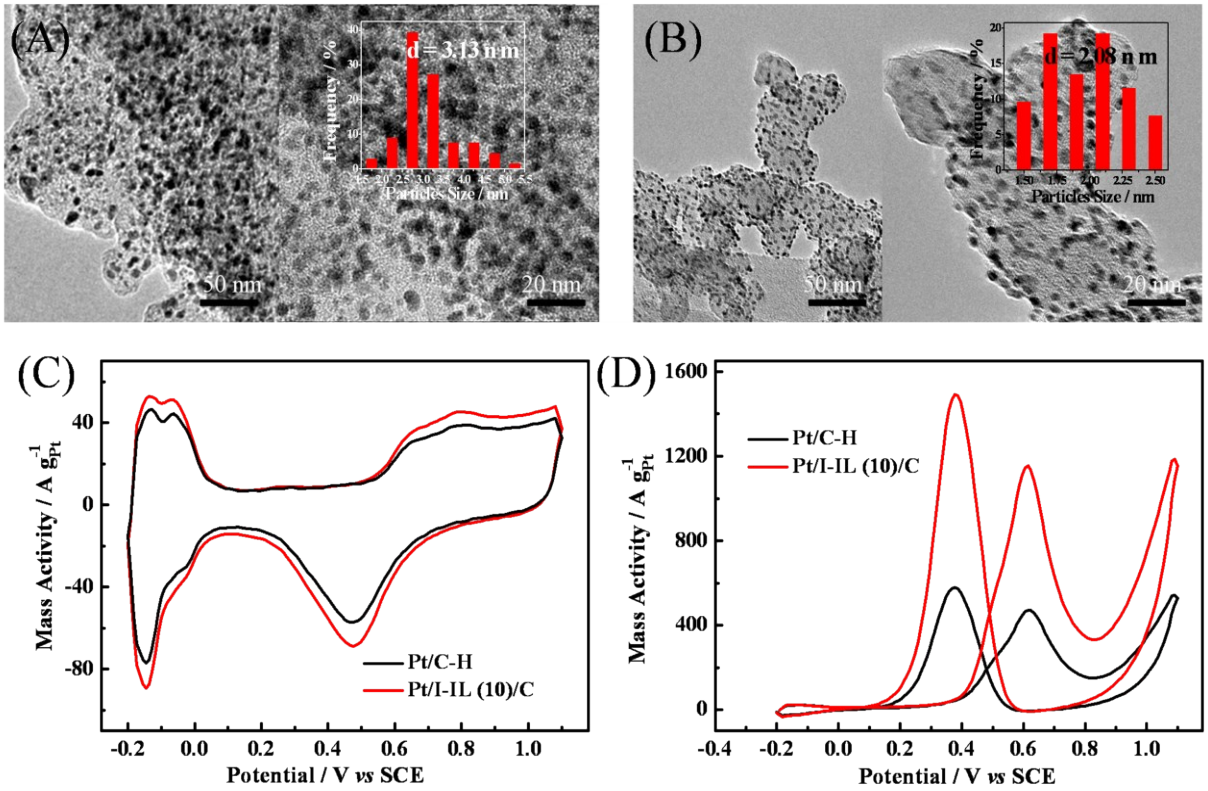


**Figure S3** TEM images of (A) Pt/C and (B) Pt/I-IL (10)/C; (C) CVs of Pt/C and Pt/I-IL (10)/C catalysts in 0.5 M nitrogen-saturated $H_2SO_4$ at a scan rate of 50 mV $S^{-1}$; (D) CVs of Pt/C-H and Pt/I-IL (10)/C catalysts in nitrogen-saturated 0.5 M $H_2SO_4$ solution containing 1.0 M $CH_3OH$ at a scan rate of 50 mV $S^{-1}$.

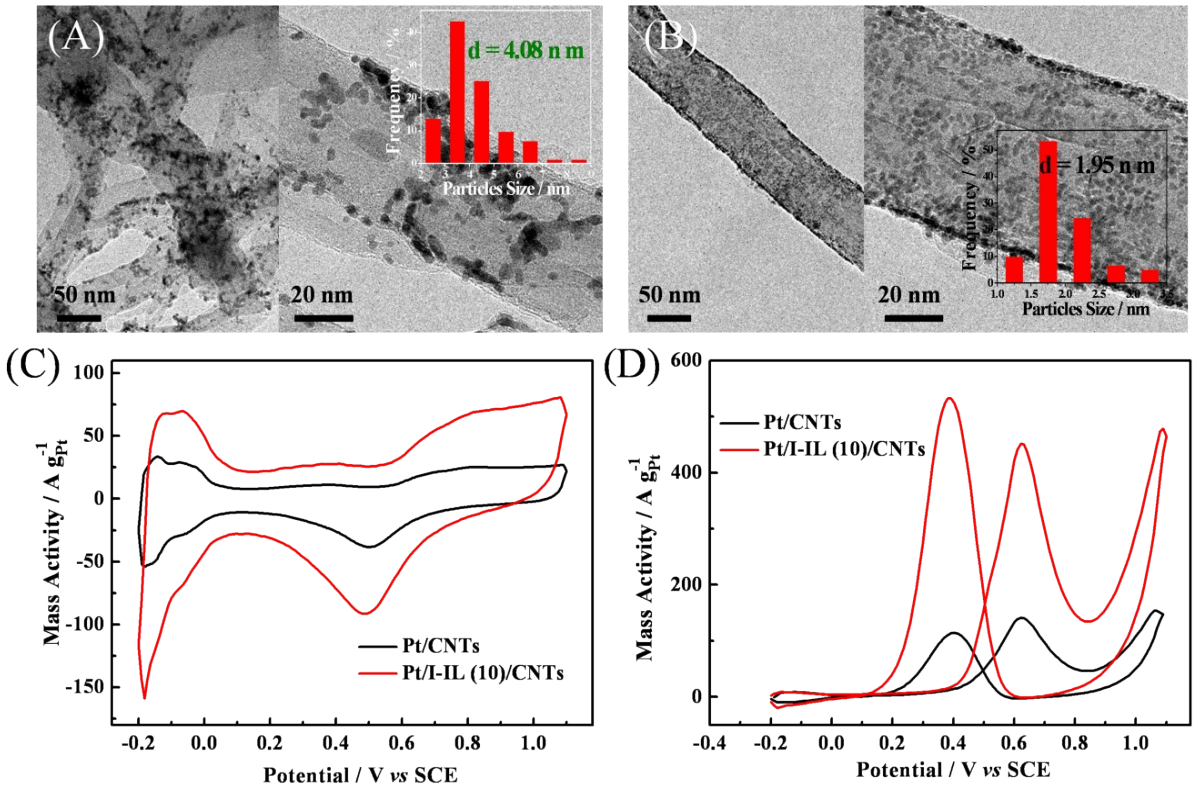


**Figure S4** TEM images of (A) Pt/CNTs and (B) Pt/I-IL (10)/CNTs; (C) CVs of Pt/CNTs and Pt/I-IL (10)/CNTs catalysts in 0.5 M nitrogen-saturated $H_2SO_4$ at a scan rate of 50 mV $S^{-1}$; (D) CVs of Pt/CNTs and Pt/I-IL (10)/CNTs catalysts in nitrogen-saturated 0.5 M $H_2SO_4$ solution containing 1.0 M $CH_3OH$ at a scan rate of 50 mV $S^{-1}$.

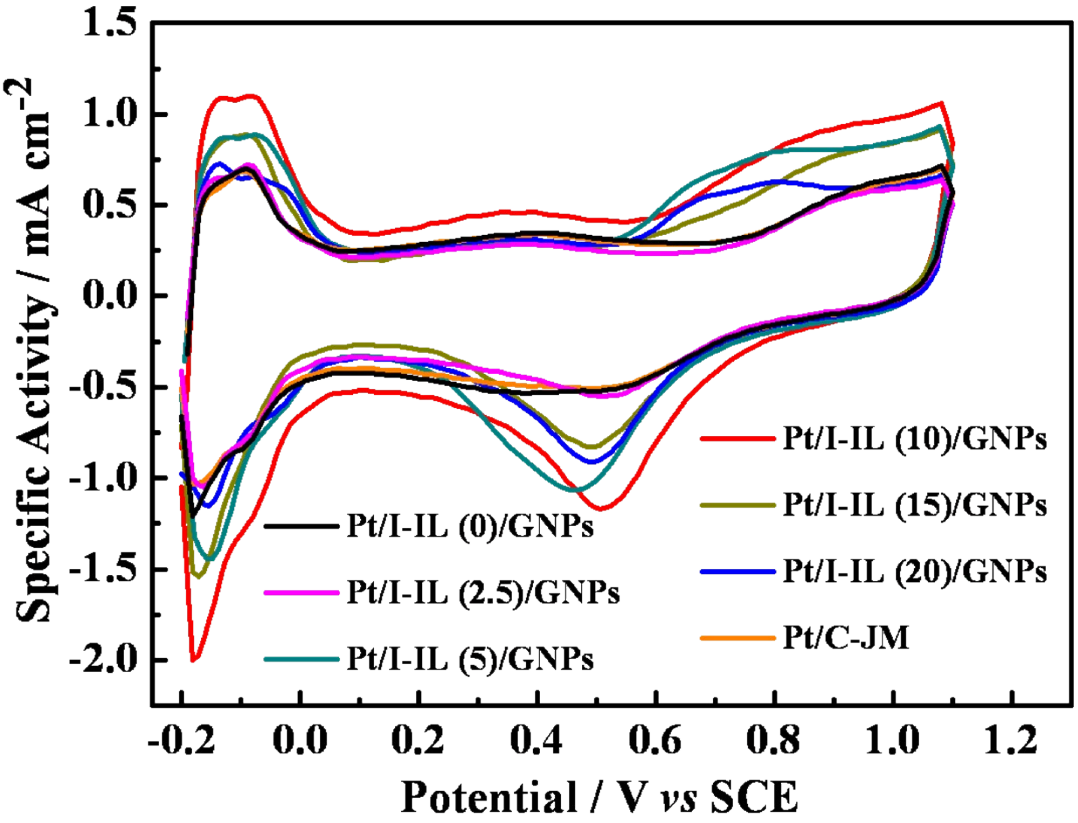


**Figure S5** Typical cyclic voltammograms of Pt/I-IL (0)/GNPs, Pt/I-IL (2.5)/GNPs, Pt/I-IL (5.0)/GNPs, Pt/I-IL (10)/GNPs, Pt/I-IL (15)/GNPs, Pt/I-IL (20)/GNPs and Pt/C-JM catalysts in 0.5 M nitrogen-saturated $H_2SO_4$ at a scan rate of 50 mV $S^{-1}$.

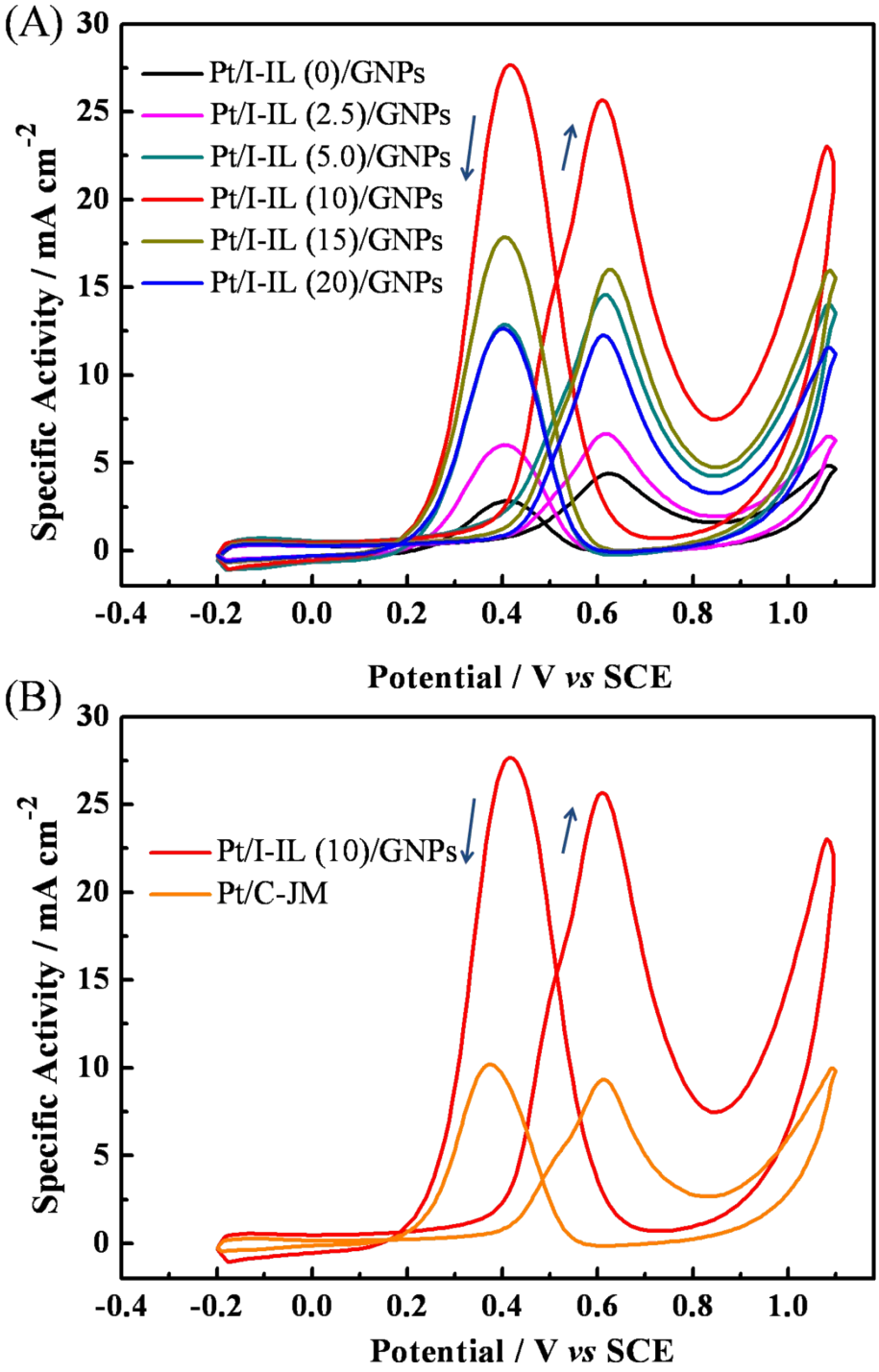


**Figure S6** The specific activity of Pt/I-IL (x)/GNPs catalysts employed in this work illustrated by the cyclic voltammograms in a 0.5 M $H_2SO_4$ solution containing 1 M methanol at a scan rate of 50 mV $s^{-1}$.

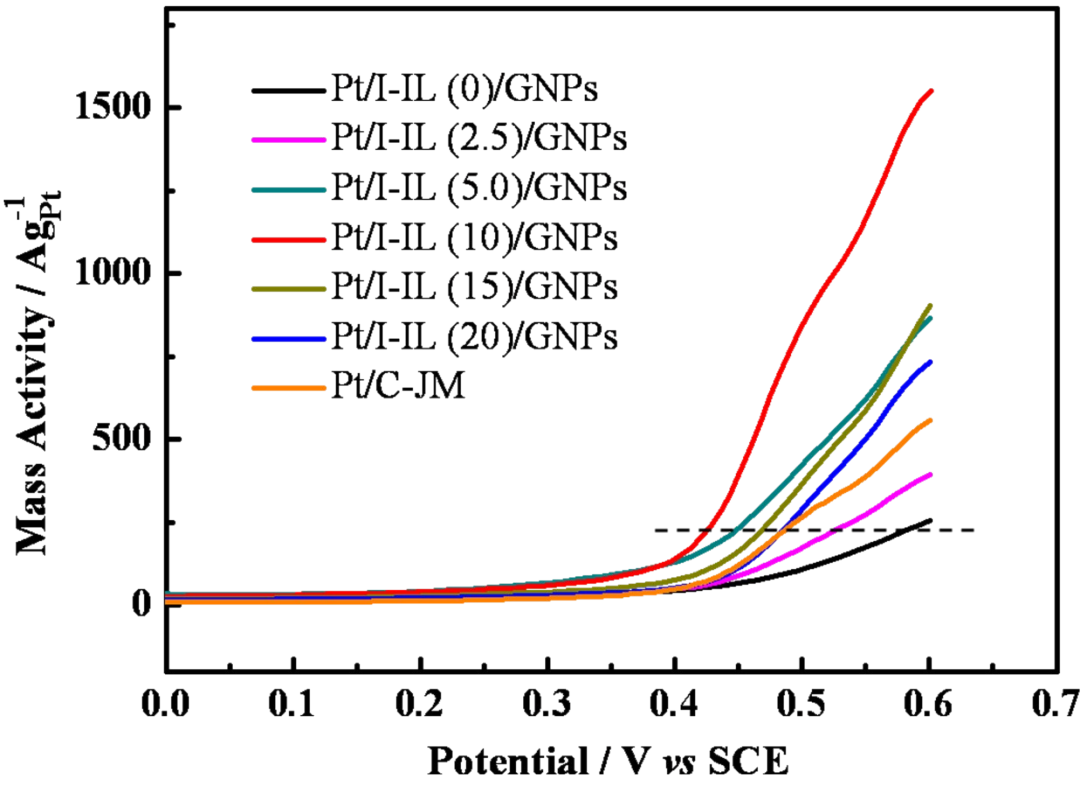


**Figure S7** Linear sweep voltammetry of Pt/I-IL (x)/GNPs and Pt/C-JM catalysts in a 0.5 M $H_2SO_4$ solution containing 1.0 M methanol at the scan rate of 50 mV $s^{-1}$.

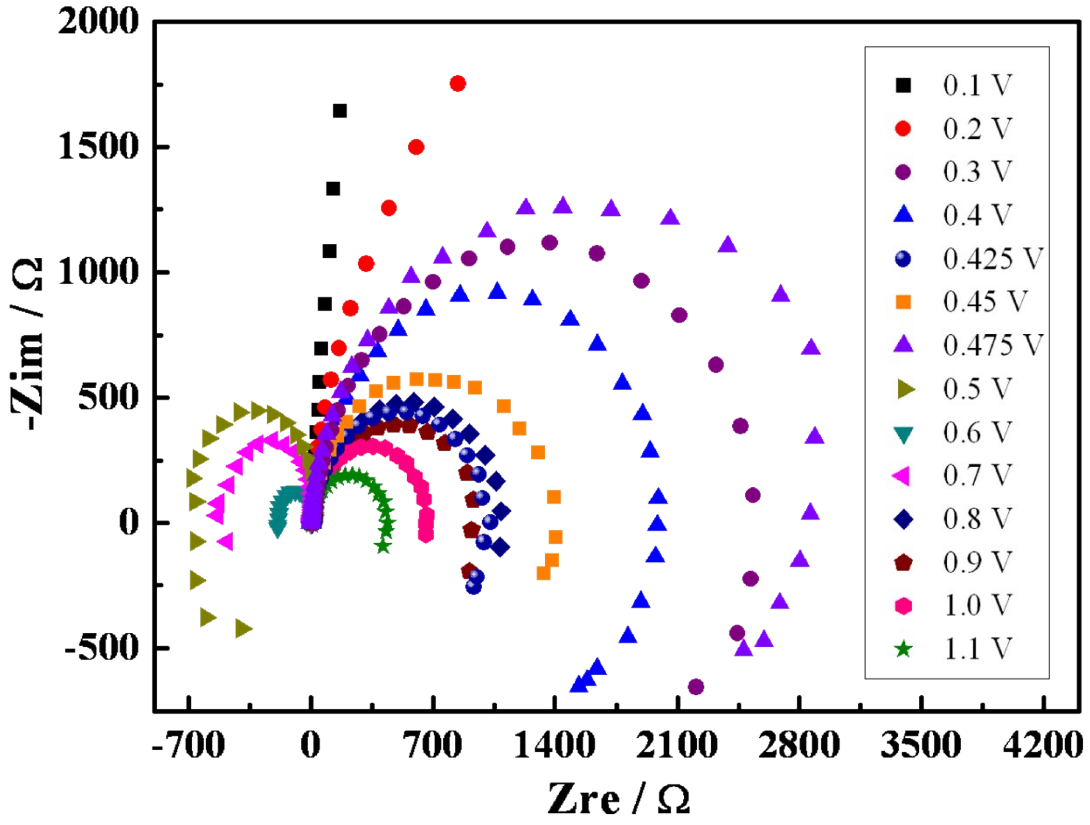


**Figure S8** Nyquist plots for the Pt/I-IL (10)/GNPs catalyst in electrochemical methanol oxidation at different potential.

## References


[1] B. Ma, J. Bai, L. Dong, *J. Solid State Electr.*, 2013, **17**, 2783-2788.

[2] H. Wang, H. Baltruschat, *J. Phys. Chem. C*, 2007, **111**, 7038-7048.

[3] M. E. Orazem, B. Tribollet, *Electrochim. Acta*, 2008, **53**, 7360-7366.

[4] J. Chang, L. Feng, C. Liu, W. Xing, X. Hu, *Energy Environ. Sci.*, 2014, **7**, 1628-1632.

[5] R. Wang, Y. Xie, K. Shi, J. Wang, C. Tian, P. Shen, H. Fu, *Chem. Eur. J.*, 2012, **18**, 7443-7451.

[6] S. Guo, S. Dong, E. Wang, *ACS Nano*, 2009, **4**, 547-555.

[7] L. Wei, Y. J. Fan, J. H. Ma, L. H. Tao, R. X. Wang, J. P. Zhong, H. Wang, *J. Power Sources*, 2013, **238**, 157-164.

[8] S. Mayavan, H. S. Jang, M. J. Lee, S. H. Choi, *J. Mater. Chem. A*, 2013, **1**, 3489-3494.

[9] H. Yan, C. Tian, L. Sun, B. Wang, L. Wang, J. Yin, A. Wu, H. Fu, *Energy Environ. Sci.*, 2014, **7**, 1939-1949.

[10] G. Chen, Y. Tan, B. Wu, G. Fu, N. Zheng, *Chem. Commun.*, 2012, **48**, 2758-2760.

[11] Y. Y. Chu, Z. B. Wang, J. Cao, D. M. Gu, G. P. Yin, *Fuel Cells*, 2013, **13**, 380-386.

[12] Y. Hu, H. Zhang, P. Wu, H. Zhang, B. Zhou, C. Cai, *Phys. Chem. Chem.l Phys.*, 2011, **13**, 4083-4094.

[13] J. Zhao, H. Yu, Z. Liu, M. Ji, L. Zhang, G. Sun, *J. Phys. Chem. C*, 2014, **118**, 1182-1190.

[14] Y. G. Zhou, J. J. Chen, F. B. Wang, Z. H. Sheng, X. H. Xia, *Chem. Commun.*, 2010, **46**, 5951-5953.

[15] B. Wu, D. Hu, Y. Kuang, B. Liu, X. Zhang, J. Chen, *Angew. Chem. Int. Edit.*, 2009, **48**, 4751-4754.